Commun. Comput. Phys.
doi: 10.4208/cicp.071009.160310s

Vol. **9**, No. 3, pp. 587-606
March 2011

A Least-Squares/Fictitious Domain Method for Linear Elliptic Problems with Robin Boundary Conditions

Roland Glowinski[1,2] and Qiaolin He[3,4,*]

[1] *Department of Mathematics, University of Houston, Houston, TX 77204, USA.*
[2] *Institute of Advanced Study, The Hong Kong University of Science and Technology, Clear Water Bay, Kowloon, Hong Kong.*
[3] *Department of Mathematics, The Hong Kong University of Science and Technology, Clear Water Bay, Kowloon, Hong Kong.*
[4] *Department of Mathematics, Sichuan University, Chengdu 610064, China.*

Received 7 October 2009; Accepted (in revised version) 16 March 2010

Available online 17 September 2010

To the memory of David Gottlieb

Abstract. In this article, we discuss a least-squares/fictitious domain method for the solution of linear elliptic boundary value problems with Robin boundary conditions. Let Ω and ω be two bounded domains of $\mathbf{R}^d$ such that $\overline{\omega}\subset\Omega$. For a linear elliptic problem in $\Omega\backslash\overline{\omega}$ with Robin boundary condition on the boundary γ of ω, our goal here is to develop a fictitious domain method where one solves a variant of the original problem on the full Ω, followed by a well-chosen correction over ω. This method is of the virtual control type and relies on a least-squares formulation making the problem solvable by a conjugate gradient algorithm operating in a well chosen control space. Numerical results obtained when applying our method to the solution of two-dimensional elliptic and parabolic problems are given; they suggest optimal order of convergence.

AMS subject classifications: 65M85, 65N85, 76M10, 93E24

Key words: Least-Square methods, fictitious domain methods, finite element methods, Robin boundary conditions.

1 Introduction

Fictitious domain methods for the solution of partial differential equations are very useful methods for the solution of complicated problems. To the best of our knowledge, these methods have been introduced by Hyman [1] and further investigated by many authors;

*Corresponding author. *Email addresses:* `roland@math.uh.edu` (R. Glowinski), `hqlaa@ust.hk` (Q. He)

let us mention, among others, Saul'ev [2,3] and Buzbee, Dorr, George and Golub [4]. In Glowinski, Pan and Periaux [5–7] and Glowinski, Pan, Kearsley and Periaux [8], fictitious domain methods were discussed for the solution of Dirichlet problems, the Dirichlet boundary condition being enforced as a side constraint, using a *boundary supported Lagrange multiplier*. A volume-supported Lagrange multiplier based fictitious domain method was introduced in Glowinski, Pan, Hesla, Joseph and Periaux in [9], the main motivation of these authors being the direct numerical simulation of particulate flow when the number of particles exceeds 10^3. Initially tested on particulate flow with spherical particles, the method discussed in [9] was generalized to situations involving particles with more complicated shapes, as shown for example in Pan, Glowinski and Galdi [10].

The main idea behind fictitious domain methods is to extend a problem initially posed on a geometrically complex shaped domain to a larger simpler domain; this provides two main advantages when constructing numerical schemes: (i) the extended domain is geometrically simpler and allows the use of fast solvers. (ii) The same fixed mesh can be used for the entire computation, eliminating thus the need for repeated re-meshing and projection. All the studies that we know of, concerning the application of fictitious domain methods to the simulation of particulate flow, consider no-slip boundary conditions at the interface between fluid and particles. There are situations however, in *micro-fluidics* for example, where a slip condition on the particle surface is more realistic than the no-slip one. If the no-slip boundary condition on the particle surface is replaced by the Navier slip boundary condition, the volume-supported Lagrange multiplier based fictitious domain methods discussed in [5–10], which rely on H^1-extensions, are not easy to generalize to the slip situation.

The main goal of the present article is to discuss the solution of linear elliptic boundary value problems with *Robin boundary conditions*; we see this as a first step to the construction of fictitious domain methods suited to slip boundary conditions. The method is of the *virtual control* type (in the sense of J. L. Lions; see [11]) and relies on a *least-squares* formulation making the problem solvable by a *conjugate gradient* algorithm operating in a well-chosen control space.

The formulation of the boundary value problems is given in Section 2. In Section 3, we describe a least-squares/fictitious domain method for the solution of linear elliptic problems with Robin boundary conditions. In Section 4, we discuss the conjugate gradient solution of the least-squares problems introduced in Section 3. The *finite element* implementation of the above methodology is discussed in Section 5. Finally, we present in Section 6 the results of numerical experiments; in particular, these results suggest optimal order of convergence for various norms of the approximation error.

A (brief) history of *fictitious domain methods* can be found in, e.g., [12, Chapter 8].

2 Formulation of the boundary value problems

Let Ω and ω be two bounded domains of $\mathbf{R}^d$, such that $d \geq 1$ and $\overline{\omega} \subset \Omega$ (see Fig. 1). We denote by Γ and γ the boundaries of Ω and ω, respectively.

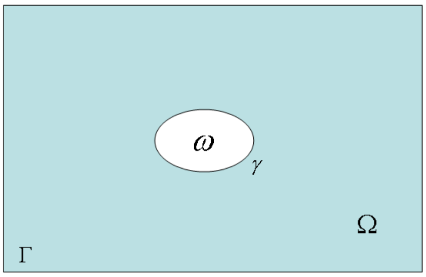

Figure 1: Problem geometry.

The *Robin-Dirichlet* problem under consideration reads as follows:

$$\alpha\psi-\mu\nabla^2\psi=f, \qquad \text{in } \Omega\backslash\overline{\omega}, \tag{2.1a}$$

$$\psi=g_0, \qquad \text{on } \Gamma, \tag{2.1b}$$

$$\mu\Big(\frac{\partial\psi}{\partial n}+\frac{\psi}{l_s}\Big)=g_1, \quad \text{on } \gamma, \tag{2.1c}$$

where α (resp. μ) is a non-negative (resp. a positive) constant, $f\in L^2(\Omega\backslash\overline{\omega})$, $g_0\in H^{3/2}(\Gamma)$, $g_1\in H^{1/2}(\gamma)$, $\mathbf{n}$ is the unit normal vector at γ pointing outward of $\Omega\backslash\overline{\omega}$ and l_s is a characteristic distance. We assume that Ω is convex (or has a smooth boundary) and that γ is smooth. Problem (2.1) has a unique solution in $H^2(\Omega\backslash\overline{\omega})$ which is also the solution of the following linear variational problem:

$$\psi\in H^1(\Omega\backslash\overline{\omega}), \quad \psi=g_0, \quad \text{on } \Gamma, \tag{2.2a}$$

$$\alpha\int_{\Omega\backslash\overline{\omega}}\psi\varphi dx+\mu\int_{\Omega\backslash\overline{\omega}}\nabla\psi\cdot\nabla\varphi dx+\frac{\mu}{l_s}\int_\gamma\psi\varphi d\gamma$$
$$=\int_{\Omega\backslash\overline{\omega}}f\varphi dx+\int_\gamma g_1\varphi d\gamma, \quad \forall\varphi\in V_0, \tag{2.2b}$$

where $dx=dx_1\cdots dx_d$ and $V_0=\{\varphi|\varphi\in H^1(\Omega\backslash\overline{\omega}),\ \varphi=0, \text{ on } \Gamma\}$.

3 A least-squares/ fictitious domain method for (2.1) and (2.2)

3.1 A fictitious domain formulation of problems (2.1) and (2.2)

We proceed as follows to define a *fictitious domain* variant of problems (2.1) and (2.2):

(i) To $v\in L^2(\omega)$ we associate $\widetilde{f}(v)$ defined by

$$\widetilde{f}(v)\in L^2(\Omega), \qquad \widetilde{f}(v)|_{\Omega\backslash\overline{\omega}}=f, \qquad \widetilde{f}(v)|_\omega=v, \tag{3.1}$$

and then the solution $\{\psi_1,\psi_2\}$ of the following elliptic system

$$\alpha\psi_1-\mu\nabla^2\psi_1=\widetilde{f}(v), \quad \text{in } \Omega, \qquad \psi_1=g_0, \qquad \text{on } \Gamma, \tag{3.2a}$$

$$\alpha\psi_2-\mu\nabla^2\psi_2=v, \qquad \text{in } \omega, \qquad \mu\frac{\partial\psi_2}{\partial n}=\frac{\mu}{l_s}\psi_1-g_1, \quad \text{on } \gamma. \tag{3.2b}$$

Both problems (3.2a) and (3.2b) have a unique solution in $H^1(\Omega)$ and $H^1(\omega)$, respectively (actually, ψ_1 and ψ_2 have both the H^2-regularity).

(ii) We define $\mathbf{A}:L^2(\omega)\to H^1(\omega)$ by

$$\mathbf{A}(v)=(\psi_2-\psi_1)|_\omega, \tag{3.3}$$

operator $\mathbf{A}$ is clearly *affine* and *continuous*.

(iii) We observe that if v verifies $\mathbf{A}(v)=0$, then $\psi_2=\psi_1$ on ω and it is easy to see that the H^2-regularity of ψ_1 and ψ_2 implies that $\psi_1|_{\Omega\setminus\overline{\omega}}=\psi$, where ψ is the solution of problems (2.1) and (2.2). We still have to show that indeed the functional equation

$$\mathbf{A}(u)=0 \tag{3.4}$$

has a solution and to discuss is numerical solution. In that direction, we are going to prove the following.

Theorem 3.1. *The functional equation* (3.4) *has a solution.*

Proof. We prove the existence by constructing such a solution. Due to the H^2-regularity of the solution ψ to problem (2.1), we have

$$\psi|_\gamma\in H^{\frac{3}{2}}(\gamma). \tag{3.5}$$

Since $g_1\in H^{1/2}(\gamma)$, there exists an infinity of functions $\theta\in H^2(\omega)$ such that

$$\theta|_\gamma=\psi|_\gamma, \qquad \frac{\partial\theta}{\partial n}=\frac{\psi}{l_s}-\frac{g_1}{\mu}, \quad \text{on } \gamma. \tag{3.6}$$

One of these functions θ is the unique solution in $H^2(\omega)$ of the following linear biharmonic boundary value problem:

$$\nabla^4\theta=0, \quad \text{in } \omega, \quad \theta|_\gamma=\psi|_\gamma, \quad \frac{\partial\theta}{\partial n}=\frac{\psi}{l_s}-\frac{g_1}{\mu}, \quad \text{on } \gamma. \tag{3.7}$$

Consider $\theta\in H^2(\omega)$ verifying (3.6); from θ define u_θ by

$$u_\theta=\alpha\theta-\mu\nabla^2\theta. \tag{3.8}$$

The $H^2(\omega)$-regularity of θ implies that $u_\theta \in L^2(\omega)$. Next, we define $\widetilde{f}(u_\theta), \psi_1$ and ψ_2 by

$$\widetilde{f}(u_\theta)=f, \quad \text{in } \Omega\backslash\overline{\omega} \quad \text{and} \quad \widetilde{f}(u_\theta)=u_\theta, \quad \text{in } \omega, \tag{3.9a}$$

$$\psi_1=\psi, \quad \text{in } \Omega\backslash\overline{\omega} \quad \text{and} \quad \psi_1=\theta, \quad \text{in } \omega, \tag{3.9b}$$

$$\psi_2=\theta, \quad \text{in } \omega. \tag{3.9c}$$

Since ψ and $\partial\psi/\partial n$ match, respectively, θ and $\partial\theta/\partial n$ on γ, the function ψ_1 defined by (3.9b) belongs to $H^2(\Omega)$. Thus ψ_1 and ψ_2 in (3.9b) and (3.9c) satisfy (3.2a) and (3.2b) for $v=u_\theta$ and

$$\mathbf{A}(u_\theta)=0.$$

This concludes the proof of the theorem. □

Remark 3.1. Problem (3.4) can be viewed as an exact controllability problem in the sense of [13]. From a practical point of view, problem (3.4) has an infinity of solutions. If a conjugate gradient algorithm is applied to a least-squares variant of (3.4) with 0 as initial guess, we can expect convergence to the unique solution of problem (3.4) of minimal norm in $L^2(\omega)$.

Remark 3.2. If there exists a "natural" extension $\widetilde{f}$ of f over Ω (that is, $\widetilde{f}\in L^2(\Omega)$ and $f=\widetilde{f}\,|_{\Omega\backslash\overline{\omega}}$) we can replace $\widetilde{f}(v)$ in (3.1) by $\widetilde{f}+v\chi_\omega$. This will modify slightly the least-squares formulation and conjugate gradient algorithm to be discussed in the following parts of this article.

3.2 A least-squares formulation of problem (3.4)

A "reasonable" least-squares formulation of problem (3.4) reads as follows: find $u\in L^2(\omega)$, such that

$$J(u)\le J(v), \quad \forall v\in L^2(\omega), \tag{3.10}$$

with

$$J(v)=\frac{1}{2}\int_\omega \left[\alpha|\psi_2-\psi_1|^2+\mu|\nabla(\psi_2-\psi_1)|^2\right]dx, \tag{3.11}$$

where ψ_1 and ψ_2 are the respective solutions in $H^2(\Omega)$ and $H^2(\omega)$ of

$$\alpha\psi_1-\mu\nabla^2\psi_1=\widetilde{f}(v), \quad \text{in } \Omega, \qquad \psi_1=g_0, \qquad \text{on } \Gamma, \tag{3.12a}$$

$$\alpha\psi_2-\mu\nabla^2\psi_2=v, \qquad \text{in } \omega, \qquad \mu\frac{\partial\psi_2}{\partial n}=\frac{\mu}{l_s}\psi_1-g_1, \quad \text{on } \gamma. \tag{3.12b}$$

The functional J is clearly convex and C^∞ over $L^2(\omega)$. Any solution of problem (3.4) is a solution of the minimization problem (of the *virtual control* type) (3.10). Such a solution is characterized by

$$DJ(u)=0, \tag{3.13}$$

where $DJ(\cdot)$ is the differential of the functional J. Since the conjugate gradient solution of the least-squares problem (3.10) will require $DJ(.)$, we will dedicate the next section to the computation of $DJ(v)$, for v arbitrary in $L^2(\omega)$.

3.3 On the computation of $DJ(v)$

Let us consider $v\in L^2(\omega)$; since $L^2(\omega)$ is a Hilbert space, it makes sense to look for $DJ(v)$ also in $L^2(\omega)$. To compute $DJ(v)$ we will use a *perturbation* method. Let δv be a perturbation of v; we have then

$$\begin{aligned}\delta J(v)&=\int_\omega DJ(v)\delta v dx\\&=\int_\omega\big[\alpha(\psi_2-\psi_1)\delta(\psi_2-\psi_1)+\mu\nabla(\psi_2-\psi_1)\cdot\nabla\delta(\psi_2-\psi_1)\big]dx,\end{aligned} \tag{3.14}$$

with $\delta\psi_2$ and $\delta\psi_1$ satisfying

$$\alpha\delta\psi_1-\mu\nabla^2\delta\psi_1=\delta v\chi_\omega,\quad \text{in } \Omega,\qquad \delta\psi_1=0,\qquad \text{on } \Gamma, \tag{3.15a}$$

$$\alpha\delta\psi_2-\mu\nabla^2\delta\psi_2=\delta v,\quad \text{in } \omega,\qquad \mu\frac{\partial}{\partial n}\delta\psi_2=\frac{\mu}{l_s}\delta\psi_1,\quad \text{on } \gamma, \tag{3.15b}$$

χ_ω being the *characteristic function* of ω (that is $\chi_\omega(x)=1$ if $x\in\omega,\chi_\omega(x)=0$ elsewhere). We introduce now $p_1\in H_0^1(\Omega)$; multiplying both sides of (3.15a) by p_1 and integrating by parts, we obtain

$$\int_\Omega\big[\alpha p_1\delta\psi_1+\mu\nabla p_1\cdot\nabla\delta\psi_1\big]dx=\int_\omega p_1\delta v dx. \tag{3.16}$$

Similarly, if we multiply both sides of (3.15b) by $\psi_2-\psi_1$, we obtain

$$\begin{aligned}&\int_\omega\big[\alpha(\psi_2-\psi_1)\delta\psi_2+\mu\nabla(\psi_2-\psi_1)\cdot\nabla\delta\psi_2\big]dx\\=&\frac{\mu}{l_s}\int_\gamma(\psi_2-\psi_1)\delta\psi_1 d\gamma+\int_\omega(\psi_2-\psi_1)\delta v dx.\end{aligned} \tag{3.17}$$

Suppose that p_1 is solution (necessarily unique) to the following Dirichlet problem (written in variational form): find $p_1\in H_0^1(\Omega)$, verifying

$$\begin{aligned}\int_\Omega\big[\alpha p_1\varphi+\mu\nabla p_1\cdot\nabla\varphi\big]dx=&\int_\omega\big[\alpha(\psi_1-\psi_2)\varphi+\mu\nabla(\psi_1-\psi_2)\cdot\nabla\varphi\big]dx\\&+\frac{\mu}{l_s}\int_\gamma(\psi_2-\psi_1)\varphi d\gamma,\quad \forall\varphi\in H_0^1(\Omega).\end{aligned} \tag{3.18}$$

Since $\delta\psi_1 \in H_0^1(\Omega)$, it follows from (3.14) and (3.16)-(3.18) that

$$\delta J(v) = \int_\omega DJ(v)\delta v dx = \int_\omega (p_1 + \psi_2 - \psi_1)\delta v dx,$$

which implies

$$DJ(v) = (p_1 - \psi_1)|_\omega + \psi_2. \tag{3.19}$$

Thus, in order to compute $DJ(v)$, we first compute ψ_1 from (3.1) and (3.2a), then ψ_2 from (3.2b) and p_1 from (3.18). Finally, we obtain $DJ(v)$ from (3.19).

4 On the conjugate gradient solution of the least-squares problem (3.10)

4.1 Generalities

In order to solve the (linear) least-squares problem (3.10), we advocate a *conjugate gradient* algorithm operating in the Hilbert space $L^2(\omega)$. Such algorithms and many applications are discussed in Glowinski [12]. Let us consider the following generic optimization problem

$$u \in H \quad \text{and} \quad j(u) \leq j(v), \quad \forall v \in H, \tag{4.1}$$

where: (i) H is a real Hilbert space with the scalar product $(\cdot,\cdot)$ and the associated norm $\|\cdot\|$, and (ii) j is differentiable. Assuming that the minimization problem (4.1) has a solution, then this solution satisfies

$$Dj(u) = 0. \tag{4.2}$$

In order to solve (4.1) via (4.2), we advocate the following *conjugate gradient algorithm*, operating in the space H (we denote by $<.,.>$ the pairing between H' and H, H' being the dual space of H):

$$u^0 \text{ is given in } H; \tag{4.3}$$

solve

$$\begin{aligned} &g^0 \in H, \\ &(g^0, v) = \langle Dj(u^0), v\rangle, \quad \forall v \in H, \end{aligned} \tag{4.4}$$

and set

$$w^0 = g^0. \tag{4.5}$$

For $n\geq 0$, assuming that u^n,g^n and w^n are known, compute u^{n+1},g^{n+1} and w^{n+1} as follows: solve

$$\begin{aligned}&\rho_n\in\mathbf{R},\\&j(u^n-\rho_n w^n)\leq j(u^n-\rho w^n),\quad \forall\rho\in\mathbf{R},\end{aligned}\tag{4.6}$$

compute

$$u^{n+1}=u^n-\rho_n w^n,\tag{4.7}$$

and solve

$$\begin{aligned}&g^{n+1}\in H,\\&(g^{n+1},v)=\langle Dj(u^{n+1}),v\rangle,\quad \forall v\in H.\end{aligned}\tag{4.8}$$

If $\|g^{n+1}\|/\|g^0\|\leq tol$, take $u=u^{n+1}$; else compute

$$\gamma_n=\frac{\|g^{n+1}\|^2}{\|g^n\|^2},\tag{4.9}$$

and set

$$w^{n+1}=g^{n+1}+\gamma_n w^n.\tag{4.10}$$

Do $n+1\rightarrow n$ and return to (4.6).

4.2 Application of the conjugate gradient algorithms (4.3)-(4.10) to the solution of the least-squares problem (3.10)

Applying algorithms (4.3)-(4.10), with $H=L^2(\omega)$, to the solution of problem (3.10), we obtain (from the linearity of problem (3.13) and the fact that we identify $L^2(\omega)$ to its dual space):

$$u^0 \text{ is given in } L^2(\omega),\tag{4.11}$$

solve the following elliptic boundary value problems

$$\begin{aligned}&\psi_1^0\in H^1(\Omega),\\&\alpha\psi_1^0-\mu\nabla^2\psi_1^0=\widetilde{f}(u^0),\quad \text{in }\Omega\quad\text{and}\quad \psi_1^0=g_0,\quad\text{on }\Gamma,\end{aligned}\tag{4.12a}$$

$$\begin{aligned}&\psi_2^0\in H^1(\omega),\\&\alpha\psi_2^0-\mu\nabla^2\psi_2^0=u^0,\quad \text{in }\omega\quad\text{and}\quad \mu\frac{\partial\psi_2^0}{\partial n}=\frac{\mu}{l_s}\psi_1^0-g_1,\quad\text{on }\gamma,\end{aligned}\tag{4.12b}$$

$$\begin{aligned}&p_1^0\in H_0^1(\Omega),\\&\int_\Omega\left[\alpha p_1^0\varphi+\mu\nabla p_1^0\cdot\nabla\varphi\right]dx=\int_\omega\left[\alpha(\psi_1^0-\psi_2^0)\varphi+\mu\nabla(\psi_1^0-\psi_2^0)\cdot\nabla\varphi\right]dx\\&\qquad\qquad+\frac{\mu}{l_s}\int_\gamma(\psi_2^0-\psi_1^0)\varphi d\gamma,\quad\forall\varphi\in H_0^1(\Omega),\end{aligned}\tag{4.12c}$$

and set

$$g^0=(p_1^0-\psi_1^0)|_\omega+\psi_2^0, \qquad w^0=g^0. \tag{4.13}$$

For $n\geq 0$, assuming that u^n,g^n and w^n are known, the last two different from 0, we compute u^{n+1},g^{n+1} and w^{n+1} as follows: solve

$$\begin{aligned}
&\overline{\psi}_1^n\in H_0^1(\Omega),\\
&\alpha\overline{\psi}_1^n-\mu\nabla^2\overline{\psi}_1^n=w^n\chi_\omega, \quad \text{in } \Omega \quad \text{and} \quad \overline{\psi}_1^n=0, \quad \text{on } \Gamma,
\end{aligned} \tag{4.14a}$$

$$\begin{aligned}
&\overline{\psi}_2^n\in H^1(\omega),\\
&\alpha\overline{\psi}_2^n-\mu\nabla^2\overline{\psi}_2^n=w^n, \quad \text{in } \omega \quad \text{and} \quad \mu\frac{\partial\overline{\psi}_2^n}{\partial n}=\frac{\mu}{l_s}\overline{\psi}_1^n, \quad \text{on } \gamma,
\end{aligned} \tag{4.14b}$$

$$\begin{aligned}
&\overline{p}_1^n\in H_0^1(\Omega),\\
&\int_\Omega[\alpha\overline{p}_1^n\varphi+\mu\nabla\overline{p}_1^n\cdot\nabla\varphi]dx=\int_\omega[\alpha(\overline{\psi}_1^n-\overline{\psi}_2^n)\varphi+\mu\nabla(\overline{\psi}_1^n-\overline{\psi}_2^n)\cdot\nabla\varphi]dx\\
&\qquad\qquad+\frac{\mu}{l_s}\int_\gamma(\overline{\psi}_2^n-\overline{\psi}_1^n)\varphi d\gamma, \quad \forall\varphi\in H_0^1(\Omega),
\end{aligned} \tag{4.14c}$$

and set

$$\overline{g}^n=(\overline{p}_1^n-\overline{\psi}_1^n)|_\omega+\overline{\psi}_2^n. \tag{4.15}$$

Next, compute

$$\rho_n=\frac{\int_\omega|g^n|^2dx}{\int_\omega\overline{g}^nw^ndx}, \tag{4.16a}$$

$$u^{n+1}=u^n-\rho_nw^n, \qquad g^{n+1}=g^n-\rho_n\overline{g}^n. \tag{4.16b}$$

If

$$\frac{\int_\omega|g^{n+1}|^2dx}{\int_\omega|g^0|^2dx}\leq tol,$$

take $u=u^{n+1}$ and $\psi=\psi_1^{n+1}|_{\Omega\backslash\overline{\omega}}$; else compute

$$\gamma_n=\frac{\int_\omega|g^{n+1}|^2dx}{\int_\omega|g^n|^2dx}, \tag{4.17}$$

and set

$$w^{n+1}=g^{n+1}+\gamma_nw^n. \tag{4.18}$$

Do $n+1\rightarrow n$ and return to (4.14a).

Remark 4.1. If u^0 is close to u (this will be the case in the context of time dependent problems, for example) the stopping criterion we used for algorithms (4.11)-(4.18) may lead to more iterations than necessary. A more realistic stopping test is given by

$$\frac{\int_\omega|g^{n+1}|^2dx}{\max\left\{\int_\omega|g^0|^2dx,\int_\omega|u^{n+1}|^2dx\right\}}\leq tol.$$

Other stopping criteria can be used.

5 On the finite element implementation of the least-squares/fictitious domain methodology

5.1 Generalities

We describe in this section the *finite element* implementation of the least-squares/fictitious domain methodology discussed in Sections 4 and 5. We will assume that $\overline{\omega}\subset\Omega\subset\mathbf{R}^2$ and that Ω is convex and/or has a smooth boundary; similarly, we assume that γ is smooth. For simplicity we still denote by Ω and ω the polygonal approximations of the above domains. From the triangulations $\mathcal{T}_{h_1}$ of Ω and $\mathcal{T}_{h_2}$ of ω we define the following finite dimensional spaces:

$$V_{h_1}=\Big\{\varphi|\varphi\in C^0(\overline{\Omega}),\ \varphi|_T\in P_1,\ \forall T\in\mathcal{T}_{h_1}\Big\}, \tag{5.1a}$$

$$V_{0h_1}=\Big\{\varphi|\varphi\in V_{h_1},\ \varphi=0,\ \text{on}\ \Gamma\Big\}, \tag{5.1b}$$

$$V_{h_2}=\Big\{\varphi|\varphi\in C^0(\overline{\omega}),\ \varphi|_T\in P_1,\ \forall T\in\mathcal{T}_{h_2}\Big\}, \tag{5.1c}$$

P_1 being the space of the polynomials of two variables of degree ≤ 1 and h_1 (resp. h_2) the length of the largest edge(s) of the finite element triangulation $\mathcal{T}_{h_1}$ (resp. $\mathcal{T}_{h_2}$). We will use $\mathbf{h}$ to denote the two-dimensional vector $\{h_1,h_2\}$. The finite dimensional spaces V_{h_1},V_{0h_1} and V_{h_2} are finite dimensional approximations to $H^1(\Omega),H_0^1(\Omega)$ and $H^1(\omega)$, respectively. Similarly, we will use V_{h_2} to approximate the control space $L^2(\omega)$.

5.2 Finite element approximation of the least-squares problem (3.10)

To approximate the least-squares problem (3.10), we suggest

$$\begin{aligned} &u_{\mathbf{h}}\in V_{h_2},\\ &J_{\mathbf{h}}(u_{\mathbf{h}})\leq J_{\mathbf{h}}(v),\quad \forall v\in V_{h_2}, \end{aligned} \tag{5.2}$$

where

$$J_{\mathbf{h}}(v)=\frac{1}{2}\int_\omega\big[\alpha|\psi_2-\pi_2\psi_1|^2+\mu|\nabla(\psi_2-\pi_2\psi_1)|^2\big]dx. \tag{5.3}$$

In (5.3), ψ_1 is the solution of the following fully discrete approximate Dirichlet problem:

$$\begin{aligned} &\psi_1\in V_{h_1},\quad \psi_1=g_{0h_1},\quad \text{on}\ \Gamma,\\ &\int_\Omega\big[\alpha\psi_1\varphi+\mu\nabla\psi_1\cdot\nabla\varphi\big]dx=\int_\Omega f_{h_1}\varphi dx+\int_\omega v\pi_2\varphi dx,\quad \forall\varphi\in V_{0h_1}, \end{aligned} \tag{5.4}$$

where

(i) g_{0h_1} is an approximation of g_0.

(ii) $f_{h_1} \in V_{h_1}$ approximates f over $\Omega \backslash \overline{\omega}$ and vanishes at those vertices of $\mathcal{T}_{h_1}$ belonging to $\overline{\omega}$.

(iii) $\pi_2 : C^0(\overline{\Omega}) \rightarrow V_{h_2}$ is the interpolation operator defined as follows:

$$\pi_2 \varphi = \sum_{i=1}^{N_{h_2}} \varphi(Y_i) w_{2i}, \quad \forall \varphi \in C^0(\overline{\Omega}), \tag{5.5}$$

$\{Y_i\}_{i=1}^{N_{h_2}}$ being the set of the vertices of $\mathcal{T}_{h_2}$ and w_{2i} the P_1-shape function in V_{h_2} associated with the vertex Y_i (we clearly have $N_{h_2} =$ dimension of V_{h_2}).

Returning to (5.3), the function ψ_2 is the solution of the following approximate Neumann problem

$$\begin{aligned} &\psi_2 \in V_{h_2}, \\ &\int_\omega [\alpha \psi_2 \varphi + \mu \nabla \psi_2 \cdot \nabla \varphi] dx = \int_\omega v \varphi dx + \frac{\mu}{l_s} \int_\gamma (\pi_2 \psi_1 - g_{1h_2}) \varphi d\gamma, \quad \forall \varphi \in V_{h_2}, \end{aligned} \tag{5.6}$$

where g_{1h_2} is an approximation of g_1.

As its continuous analogue, the finite dimensional least-squares problem is of the *virtual control* type and is well-suited to solution by a *conjugate gradient* algorithm; a first step in this direction is the computation of the differential $DJ_{\mathbf{h}}$ of the cost functional $J_{\mathbf{h}}$, an issue to be addressed in the following section.

5.3 On the computation of $DJ_{\mathbf{h}}$

Proceeding as in Section 3.3, a perturbation analysis would show that

$$\forall v \in V_{h_2}, \quad DJ_{\mathbf{h}}(v) = \pi_2(p_1 - \psi_1) + \psi_2, \tag{5.7}$$

where $\{\psi_1, \psi_2\}$ is obtained from v via the solution of (5.4) and (5.6), and where p_1 is the solution of the following discrete Dirichlet problem

$$\begin{aligned} &p_1 \in V_{0h_1}, \\ &\int_\Omega [\alpha p_1 \varphi + \mu \nabla p_1 \cdot \nabla \varphi] dx = \int_\omega [\alpha(\pi_2 \psi_1 - \psi_2) \pi_2 \varphi + \mu \nabla (\pi_2 \psi_1 - \psi_2) \cdot \nabla \pi_2 \varphi] dx \\ &\qquad + \frac{\mu}{l_s} \int_\gamma (\psi_2 - \pi_2 \psi_1) \pi_2 \varphi d\gamma, \quad \forall \varphi \in V_{0h_1}. \end{aligned} \tag{5.8}$$

5.4 On the conjugate gradient solution of the discrete least-squares problem (5.2)

A *finite element* realization of the *conjugate gradient* algorithms (4.11)-(4.18) reads as follows:

$$u^0 \text{ is given in } V_{h_2}. \tag{5.9}$$

Solve

$$\begin{aligned}
&\psi_1^0 \in V_{h_1}, \quad \psi_1^0 = g_{0h_1}, \quad \text{on } \Gamma,\\
&\int_\Omega \left[\alpha\psi_1^0\varphi + \mu\nabla\psi_1^0\cdot\nabla\varphi\right]dx = \int_\Omega f_{h_1}\varphi dx + \int_\omega u^0\pi_2\varphi dx, \quad \forall\varphi\in V_{0h_1}, &(5.10a)\\
&\psi_2^0 \in V_{h_2},\\
&\int_\omega \left[\alpha\psi_2^0\varphi + \mu\nabla\psi_2^0\cdot\nabla\varphi\right]dx = \int_\omega u^0\varphi dx + \int_\gamma \left(\frac{\mu}{l_s}\pi_2\psi_1^0 - g_{1h_2}\right)\varphi d\gamma, \quad \forall\varphi\in V_{h_2}, &(5.10b)\\
&p_1^0 \in V_{0h_1},\\
&\int_\Omega \left[\alpha p_1^0\varphi + \mu\nabla p_1^0\cdot\nabla\varphi\right]dx = \int_\omega \left[\alpha(\pi_2\psi_1^0 - \psi_2^0)\pi_2\varphi + \mu\nabla(\pi_2\psi_1^0 - \psi_2^0)\cdot\nabla\pi_2\varphi\right]dx\\
&\qquad\qquad + \frac{\mu}{l_s}\int_\gamma (\psi_2^0 - \pi_2\psi_1^0)\pi_2\varphi d\gamma, \quad \forall\varphi\in V_{0h_1}. &(5.10c)
\end{aligned}$$

Set

$$g^0 = \pi_2(p_1^0 - \psi_1^0) + \psi_2^0, \quad w^0 = g^0. \tag{5.11}$$

Assuming that u^n,g^n and w^n are known, the last two different from 0, we compute u^{n+1},g^{n+1} and w^{n+1} as follows: find $\overline{\psi}_1^n \in V_{0h_1}$, verifying

$$\int_\Omega \left[\alpha\overline{\psi_1}^n\varphi + \mu\nabla\overline{\psi_1}^n\cdot\nabla\varphi\right]dx = \int_\omega w^n\pi_2\varphi dx, \quad \forall\varphi\in V_{0h_1}; \tag{5.12}$$

find $\overline{\psi}_2^n \in V_{h_2}$, verifying

$$\int_\omega \left[\alpha\overline{\psi}_2^n\varphi + \mu\nabla\overline{\psi}_2^n\cdot\nabla\varphi\right]dx = \int_\omega w^n\varphi dx + \frac{\mu}{l_s}\int_\gamma \pi_2\overline{\psi}_1^n\varphi d\gamma, \quad \forall\varphi\in V_{h_2}; \tag{5.13}$$

find $\overline{p}_1^n \in V_{0h_1}$, verifying

$$\begin{aligned}
\int_\Omega \left[\alpha\overline{p}_1^n\varphi + \mu\nabla\overline{p}_1^n\cdot\nabla\varphi\right]dx = &\int_\omega \left[\alpha(\pi_2\overline{\psi}_1^n - \overline{\psi}_2^n)\pi_2\varphi + \mu\nabla(\pi_2\overline{\psi}_1^n - \overline{\psi}_2^n)\cdot\nabla\pi_2\varphi\right]dx\\
&+ \frac{\mu}{l_s}\int_\gamma \left(\overline{\psi}_2^n - \pi_2\overline{\psi}_1^n\right)\pi_2\varphi d\gamma, \quad \forall\varphi\in V_{0h_1}.
\end{aligned} \tag{5.14}$$

Set

$$\overline{g}^n = \pi_2(\overline{p}_1^n - \overline{\psi}_1^n) + \overline{\psi}_2^n, \tag{5.15}$$

and compute

$$\rho_n = \frac{\int_\omega |g^n|^2 dx}{\int_\omega \overline{g}^n w^n dx}, \tag{5.16a}$$

$$u^{n+1} = u^n - \rho_n w^n, \quad g^{n+1} = g^n - \rho_n\overline{g}^n. \tag{5.16b}$$

If

$$\frac{\int_\omega |g^{n+1}|^2 dx}{\int_\omega |g^0|^2 dx} \le tol,$$

take $u = u^{n+1}$ and $\psi = \psi_1^{n+1}|_{\Omega\setminus\overline{\omega}}$; else compute

$$\gamma_n = \frac{\int_\omega |g^{n+1}|^2 dx}{\int_\omega |g^n|^2 dx} \tag{5.17}$$

and

$$w^{n+1} = g^{n+1} + \gamma_n w^n. \tag{5.18}$$

Do $n+1 \to n$ and return to (5.12).

Remark 5.1. Remark 4.1 applies also to algorithms (5.9)-(5.18).

Remark 5.2. When implementing algorithms (5.9)-(5.18), we advocate using the *trapezoidal rule* in order to compute all the L^2-scalar products and norms over Ω, ω and γ (the integrals of the form $\int_\Omega \nabla\theta\cdot\nabla\varphi dx$ or $\int_\omega \nabla\theta\cdot\nabla\varphi dx$ can (and should) be computed exactly since θ and φ are piecewise affine and continuous implying that $\nabla\theta$ and $\nabla\varphi$ are piecewise constant).

6 Numerical experiments

In this preliminary article we will focus on two-dimensional problems.

6.1 A two-dimensional elliptic problem

We consider as *first test problem* the particular case of problem (2.1) associated with

- $\Omega = (0,4)\times(0,4)$, $\omega = \{\{x_1,x_2\} \,|\, [(x_1-G_1)/a]^2 + [(x_2-G_2)/b]^2 < 1\}$ with $G_1 = G_2 = 2$, $a = 1/4$ and $b = 1/8$.
- $f(x_1,x_2) = \alpha(x_1^3 - x_2^3) - 6\mu(x_1 - x_2), \quad \forall\{x_1,x_2\} \in \Omega\setminus\overline{\omega}$.
- $g_0 = x_1^3 - x_2^3$, $g_1 = \mu[3(n_1x_1^2 - n_2x_2^2) + (x_1^3 - x_2^3)/l_s]$, $\{n_1,n_2\} = \mathbf{n}$ being the unit normal vector at γ pointing to ω.
- $\alpha = 100$, $\mu = 0.1$, $l_s = 0.1$.

The unique solution, associated with the above data, of problem (2.1) in $H^1(\Omega\setminus\overline{\omega})$, is given by

$$\psi(x_1,x_2) = x_1^3 - x_2^3.$$

Concerning the finite element implementation of the least-squares/fictitious domain discussed in the preceding sections, we employed for $\mathcal{T}_{h_1}$ (resp. $\mathcal{T}_{h_2}$) uniform triangulations

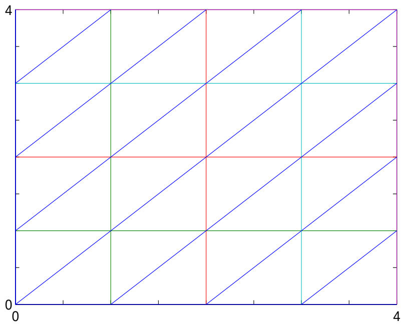

Figure 2: First test problem: a uniform triangulation of Ω.

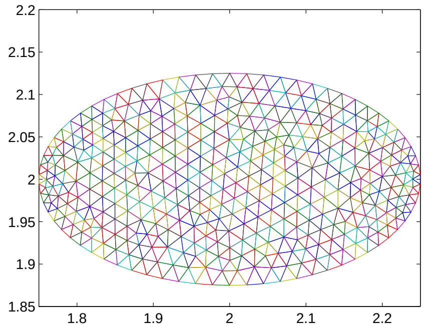

Figure 3: First test problem: a triangulation of ω.

of Ω (resp. triangulations of ω) as shown in Fig. 2 (resp. Fig. 3). We used $u^0=0$ to initialize the associated conjugate gradient algorithms (5.9)-(5.18), and took $tol=10^{-10}$ for the stopping criterion.

In Table 1, we report for $h_2=1/40$ and $h_1=1/5,1/10,1/20$ and $1/40$: (i) the number of iterations of algorithms (5.9)-(5.18) necessary to achieve convergence. (ii) The approximation error evaluated for various norms.

Table 1: First test problem: summary of numerical results ($h_2=1/40$).

h_1	Number of iterations	$\Vert\psi-\psi_h\Vert_{L^\infty(\Omega\backslash\overline{\omega})}$	$\Vert\psi-\psi_h\Vert_{L^2(\Omega\backslash\overline{\omega})}$	$\Vert\psi-\psi_h\Vert_{H^1(\Omega\backslash\overline{\omega})}$
1/5	34	0.1046	7.8370E-03	0.2855
1/10	61	2.1845E-02	1.9028E-03	0.1423
1/20	59	4.5840E-03	4.7015E-04	7.1089E-02
1/40	68	1.1385E-03	1.1708E-04	3.5518E-02

The results reported in Table 1 suggest:

- for h_1 small enough the number of iterations varies slowly with h_1.
- $\Vert\psi_{\mathbf{h}}-\psi\Vert_{L^\infty(\Omega\backslash\overline{\omega})}\approx\mathcal{O}(h_1^2)$, $\Vert\psi_{\mathbf{h}}-\psi\Vert_{L^2(\Omega\backslash\overline{\omega})}=\mathcal{O}(h_1^2)$ and $\Vert\psi_{\mathbf{h}}-\psi\Vert_{H^1(\Omega\backslash\overline{\omega})}=\mathcal{O}(h_1)$.

Concerning the decay of the cost function $J_{\mathbf{h}}$ defined by (5.3), we have, if $\mathbf{h}=\{1/10,1/40\}$ (resp. $\mathbf{h}=\{1/20,1/40\}$), $J_{\mathbf{h}}(u^0)=3.67$ (resp. $J_{\mathbf{h}}(u^0)=3.35$) and $J_{\mathbf{h}}(u^{61})=4.20\times10^{-9}$ (resp. $J_{\mathbf{h}}(u^{59})=5.11\times10^{-9}$), showing clearly that the computed approximations of ψ_1 and ψ_2 match quite well over ω.

In order to further investigate the convergence properties of the methodology discussed in the preceding sections we performed computations with $h_2=1/20$ and $h_1=1/10,1/20,1/40$ and $1/80$. The corresponding results are reported in Table 2. From these results we observe that:

- If $h_1\geq h_2$, the number of iterations necessary to achieve convergence does not vary significantly with h_1; on the other hand this number of iterations seems to increase sharply when h_1 decreases below h_2.

Table 2: First test problem: summary of numerical results ($h_2=1/20$).

h_1	Number of iterations	$\| \psi-\psi_h \|_{L^\infty(\Omega\backslash\overline{\omega})}$	$\| \psi-\psi_h \|_{L^2(\Omega\backslash\overline{\omega})}$	$\| \psi-\psi_h \|_{H^1(\Omega\backslash\overline{\omega})}$
1/10	33	2.1845E-02	1.9038E-03	0.1424
1/20	36	4.5840E-03	4.6807E-04	7.1063E-02
1/40	114	2.1385E-03	1.0163E-04	3.5434E-02
1/80	85	3.1514E-03	5.2854E-05	1.7532E-02

• The various approximation errors vary as expected (that is as in Table 1) if $h_1 \geq h_2$; on the other hand, they vary quite differently if $h_1 \leq h_2$, the only one behaving "nicely" being $\| \psi_{\mathbf{h}}-\psi \|_{H^1(\Omega\backslash\overline{\omega})}$, which shows a text-book $\mathcal{O}(h_1)$ behavior as h_1 varies over the interval [1/80,1/10]. From these results we suggest to take $h_1=h_2$ to be on the safe side.

Remark 6.1. If we compare the results obtained with $h_1=h_2=1/20$ with those associated with $h_1=h_2=1/40$, we observe that twice as many iterations are required to achieve convergence if one uses the finer meshes (suggesting a condition number of the order of h^{-2}, if we denote by h the common value of $h_1=h_2$). On the other hand, the results of Tables 1 and 2 suggest that

$$\| \psi_{\mathbf{h}}-\psi \|_{L^\infty(\Omega\backslash\overline{\omega})} \approx \mathcal{O}(h^2), \quad \| \psi_{\mathbf{h}}-\psi \|_{L^2(\Omega\backslash\overline{\omega})} = \mathcal{O}(h^2), \quad \| \psi_{\mathbf{h}}-\psi \|_{H^1(\Omega\backslash\overline{\omega})} = \mathcal{O}(h).$$

6.2 A two-dimensional parabolic problem with fixed ω

The *second test problem* is the *parabolic* one defined as follows:

$$\frac{\partial \psi}{\partial t} - \mu \nabla^2 \psi = f, \quad \text{in } (\Omega\backslash\overline{\omega}) \times (0,T), \tag{6.1a}$$

$$\psi = g_0, \quad \text{on } \Gamma \times (0,T), \quad \mu\Big(\frac{\partial \psi}{\partial n} + \frac{\psi}{l_s}\Big) = g_1, \quad \text{on } \gamma \times (0,T), \tag{6.1b}$$

$$\psi(x_1,x_2,0) = \psi_0(x_1,x_2), \tag{6.1c}$$

with

- $f(x_1,x_2,t) = (x_1^3 - x_2^3) - 6\mu(x_1-x_2)t, \quad \forall \{x_1,x_2,t\} \in (\Omega\backslash\overline{\omega}) \times (0,T)$.
- $g_0(x_1,x_2,t) = \big(x_1^3 - x_2^3\big)\, t, \quad \forall \{x_1,x_2,t\} \in \Gamma \times (0,T)$.
- $g_1(x_1,x_2,t) = \mu\big[3(n_1 x_1^2 - n_2 x_2^2) + (x_1^3 - x_2^3)/l_s\big] t, \quad \forall \{x_1,x_2,t\} \in \gamma \times (0,T)$.

The other data are as in Section 6.1. Assuming that $\psi_0 = 0$, the exact solution of problems (6.1a)-(6.1c) is given by

$$\psi(x_1,x_2,t) = (x_1^3 - x_2^3)t.$$

To time-discretize problems (6.1a)-(6.1c), we have used the following *backward Euler's scheme* (with $\Delta t(>0)$ the time-discretization step):

$$\psi^0=\psi_0; \tag{6.2}$$

for $n\geq 1$, we obtain ψ^n from ψ^{n-1} by solving the following elliptic problem

$$\frac{\psi^n-\psi^{n-1}}{\Delta t}-\mu\nabla^2\psi^n=f(n\Delta t), \quad \text{in } \Omega\backslash\overline{\omega}, \tag{6.3a}$$

$$\psi^n=g_0(n\Delta t), \quad \text{on } \Gamma, \tag{6.3b}$$

$$\mu\Big(\frac{\partial\psi^n}{\partial n}+\frac{\psi^n}{l_s}\Big)=g_1(n\Delta t), \quad \text{on } \gamma, \tag{6.3c}$$

above, $\psi(n\Delta t)$ denotes the function $\{x_1,x_2\}\rightarrow\psi(x_1,x_2,n\Delta t)$.

The fictitious domain/least-squares/finite element/conjugate gradient methodology discussed in Section 5 still applies here since problems (6.3a)-(6.3c) is clearly of the same type as the one discussed in Section 6.1. When applying the conjugate algorithms (5.9)-(5.18) to the solution of the space-discrete least-squares problem associated with (6.3a)-(6.3c) we have taken $u^0=0$ (resp. u^0 equal to the solution at the previous time step) if $n=1$ (resp. if $n\geq 2$). With this (quite natural) initialization strategy the number of conjugate gradient iterations necessary to achieve convergence drops very quickly to a small number (less than 10, typically) as n increases. The results reported in the Tables 3 and 4 have been obtained with $\Delta t=10^{-3}$. On Table 3, we have reported the results obtained at $t=1$, using $h_2=1/40$ and $h_1=1/5,1/10,1/20$ and $1/40$. From the linearity of the solution with respect to t, the approximation error is not affected by Δt. On the other hand, the approximation errors resulting from the space approximation behaves like those in Section 6.1, namely (with obvious notation): $\|\psi_{\mathbf{h}}^{\Delta t}(1)-\psi(1)\|_{L^\infty(\Omega\backslash\overline{\omega})}\approx\mathcal{O}(h_1^2)$, $\|\psi_{\mathbf{h}}^{\Delta t}(1)-\psi(1)\|_{L^2(\Omega\backslash\overline{\omega})}=\mathcal{O}(h_1^2)$ and $\|\psi_{\mathbf{h}}^{\Delta t}(1)-\psi(1)\|_{H^1(\Omega\backslash\overline{\omega})}=\mathcal{O}(h_1)$. The results reported

Table 3: Second test problem: summary of numerical results ($h_2=1/40$, $\Delta t=10^{-3}$,$t=1$).

h_1	$\|\psi-\psi_h\|_{L^\infty(\Omega\backslash\overline{\omega})}$	$\|\psi-\psi_h\|_{L^2(\Omega\backslash\overline{\omega})}$	$\|\psi-\psi_h\|_{H^1(\Omega\backslash\overline{\omega})}$
1/5	4.8078E-02	8.4802E-03	0.2841
1/10	1.1891E-02	2.1089E-03	0.1420
1/20	2.9706E-03	5.2664E-04	7.1031E-02
1/40	7.6868E-04	1.3102E-04	3.5513E-02

Table 4: Second test problem: summary of numerical results ($h_2=1/20$,$\Delta t=10^{-3}$,$t=1$).

h_1	$\|\psi-\psi_h\|_{L^\infty(\Omega\backslash\overline{\omega})}$	$\|\psi-\psi_h\|_{L^2(\Omega\backslash\overline{\omega})}$	$\|\psi-\psi_h\|_{H^1(\Omega\backslash\overline{\omega})}$
1/10	1.1891E-02	2.1097E-03	0.1421
1/20	2.9706E-03	5.2678E-04	7.1131E-02
1/40	3.0504E-03	1.3426E-04	3.5766E-02
1/80	5.5356E-03	6.9825E-05	1.8125E-02

in Table 4 lead to the same conclusions as the one in Table 2. Comparing the results in both tables we come once again to the conclusion, concerning the choice of h_1 and h_2, that the safest strategy is to take equal these two space-discretization steps.

6.3 A two-dimensional parabolic problem with moving ω

As third test problem, we consider a variant of problems (6.1a)-(6.1c) where the ellipse ω is subject to a rigid body motion obtained by the addition of a uniform translation and constant angular velocity rotation; we assume that at $t=0$, ω coincides with the ellipse encountered in Sections 6.1 and 6.2. We assume also that μ and l_s are as in Sections 6.1 and 6.2. Since $\omega(t)$ (the position occupied by the ellipse) is known in advance, we can easily construct f, g_0 and g_1 such that the exact solution will be given again by

$$\psi(x_1,x_2,t)=(x_1^3-x_2^3)t$$

(implying that, necessarily, $\psi_0=0$).

When implementing the methodology discussed in Section 5 to the solution of the moving ω variant of problems (6.1a)-(6.1c), one encounters two complications, namely:

1. When approximating $\partial\psi/\partial t$ by $(\psi^n-\psi^{n-1})/\Delta t$, we have to overcome the difficulty associated with the fact that ψ^n is defined over $\Omega\backslash\overline{\omega}(n\Delta t)$, while ψ^{n-1} is defined over $\Omega\backslash\overline{\omega}((n-1)\Delta t)$. Fortunately, our fictitious domain approach provides a simple solution to this problem, namely: replace ψ^{n-1} by $\psi_1^{n-1}|_{\Omega\backslash\overline{\omega}(n\Delta t)}$.

2. Let us denote by $u^{0,n}$ the function, belonging to $L^2(\omega)$, used to initialize the conjugate gradient algorithm for solving the least-squares problem associated with step n. When ω is fixed, we advocated in Section 6.2 the following initialization of the conjugate gradient algorithm solving the least-squares/ficititious domain problem: if $n=1$, use $u^{0,1}=0$; if $n\geq 2$, take for $u^{0,n}$ the solution u^{n-1} of the least-squares problem associated with the previous time step. If ω enjoys a rigid body motion the situation looks more complicated; to overcome the above difficulty, we suggest the following approach:

(i) Denote by $\mathbf{F}_{n-1}^n$ the rigid body displacement mapping $\omega((n-1)\Delta t)$ onto $\omega(n\Delta t)$, and denote by $\mathbf{F}_n^{n-1}$ the inverse mapping of $\mathbf{F}_{n-1}^n$.

(ii) At step n (with $n\geq 2$), initialize the conjugate gradient algorithm with $u^{0,n}$ defined by

$$u^{0,n}=u^{n-1}\circ\mathbf{F}_n^{n-1}.$$

Other possibilities exist, but the above one is the simplest, and is particularly easy to implement if the triangulation $\mathcal{T}_{h_2}$ enjoys the same rigid body motion as ω.

If Δt is small enough, the number of conjugate gradient iterations drops quickly as n increases. The numerical results obtained for various values of h_1 and h_2 have been reported in Tables 5 and 6. The results of Table 5 suggest that for h_2 given and $h_1\geq h_2$ we still have

$$\|\psi_{\mathbf{h}}-\psi\|_{L^2(\Omega\backslash\overline{\omega})}=\mathcal{O}(h_1^2) \quad \text{and} \quad \|\psi_{\mathbf{h}}-\psi\|_{H^1(\Omega\backslash\overline{\omega})}=\mathcal{O}(h_1);$$

Table 5: Third test problem: summary of numerical results ($h_2=1/40, \Delta t=10^{-3}, t=1$).

h_1	$\| \psi-\psi_h \|_{L^\infty(\Omega\setminus\overline{\omega})}$	$\| \psi-\psi_h \|_{L^2(\Omega\setminus\overline{\omega})}$	$\| \psi-\psi_h \|_{H^1(\Omega\setminus\overline{\omega})}$
1/5	4.8078E-02	8.4602E-03	0.2834
1/10	1.1891E-02	2.1054E-03	0.1417
1/20	2.9706E-03	5.3114E-04	7.0958E-02
1/40	1.3715E-03	1.4354E-04	3.5606E-02

Table 6: Third test problem: summary of numerical results ($h_2=1/20, \Delta t=10^{-3}, t=1$).

h_1	$\| \psi-\psi_h \|_{L^\infty(\Omega\setminus\overline{\omega})}$	$\| \psi-\psi_h \|_{L^2(\Omega\setminus\overline{\omega})}$	$\| \psi-\psi_h \|_{H^1(\Omega\setminus\overline{\omega})}$
1/10	1.1891E-02	2.1082E-03	0.1421
1/20	2.9807E-03	5.3120E-04	7.1158E-02
1/40	3.2653E-03	1.4435E-04	3.5788E-02
1/80	5.8054E-03	7.5073E-05	1.8267E-02

on the other hand, it seems that the error $\| \psi_{\mathbf{h}}-\psi \|_{L^\infty(\Omega\setminus\overline{\omega})}$ is still $\mathcal{O}(h_1^2)$ if $h_1 \gg h_2 = 1/40$, but is close to $\mathcal{O}(h_1)$ when h_1 gets closer to h_2. The results of Table 6 confirm the deterioration, already observed in Sections 6.1 and 6.2, of $\| \psi_{\mathbf{h}}-\psi \|_{L^\infty(\Omega\setminus\overline{\omega})}$ if $h_1 < h_2$ and strongly suggest that, as before, the safe choice is $h_1 = h_2$.

Remark 6.2. Using $\psi_1^{n-1}|_{\Omega\setminus\overline{\omega}(n\Delta t)}$ to approximate ψ^{n-1} in (6.3a) is a good strategy as long as the displacement of ω during the time interval $(n-1)\Delta t$, $n\Delta t$ is small, compared to h_1 and h_2. If Δt is fixed and we decrease h_1 and h_2 we can expect, beyond some threshold, a deterioration of the approximation errors, the first error to be affected being $\| \psi_{\mathbf{h}}-\psi \|_{L^\infty(\Omega\setminus\overline{\omega})}$, as shown by the results of Tables 5 and 6.

7 Further remarks and conclusions

Before we conclude this article, some remarks are in order:

Remark 7.1. We can easily modify the method discussed in Sections 3, 4 and 5 in order to handle other boundary conditions than Dirichlet on Γ and Robin on γ. In particular, it is very easy to treat Neumann conditions on γ.

Remark 7.2. The method discussed here is particularly robust since it has been able to handle accurately situations where ω is a rectangle, implying that $\Omega\setminus\overline{\omega}$ has re-intrant corners which in principle affects the regularity of the solutions.

Remark 7.3. In the above sections we have been assuming that Ω contains only one sub-domain ω. However, we can easily consider cases where Ω contains a large number (let us say $\geq 10^2$) sub-domains $\omega_j, j=1,\cdots,J$, possibly moving in time, as it will be the case for particulate flows, which is our main motivation for these fictitious domain related investigations.

In this article, we have discussed a fictitious domain methodology for the solution of linear elliptic problems with Robin boundary conditions. The method relies on a least-squares formulation of the virtual control type, making it well-suited for solution by a conjugate gradient algorithm operating in a well-chosen control space. Numerical experiments show that the method discussed in this article performs well for linear elliptic problems, and for linear parabolic problems as well, even when ω enjoys a rigid body motion. In a future work, we will attempt at generalizing our method to the simulation of particulate flow with a Navier slip condition at the interface fluid/particles.

Acknowledgments

The first author acknowledge the support of the Institute for Advanced Study (IAS) at The Hong Kong University of Science and Technology. The work is partially supported by grants from RGC CA05/06.SC01 and RGC-CERG 603107. The authors thank the anonymous referee for his helpful comments and suggestions.

References

[1] M. A. Hyman, Non-iterative numerical solution of boundary value problems, Appl. Sci. Res. Sec., B2 (1952), 325–351.
[2] V. K. Saul'ev, On a method for automatization of solution of boundary value problems on high performance computers, Dokl. Acad. Sci. USSB., 144(3) (1962), 497–500.
[3] V. K. Saul'ev, On the solution of some boundary value problems on high performance computers by fictitious domain methods, Siberian J. Math., 4(4) (1963), 912–925.
[4] B. L. Buzbee, F. W. Dorr, J. A. George and G. H. Golub, The direct numerical solution of the discrete Poisson equation on irregular regions, SIAM J. Numer. Anal., 8 (1971), 722–736.
[5] R. Glowinski, T. W. Pan and J. Periaux, A fictitious domain method for Dirichlet problems and applications, Comput. Methods. Appl. Mech. Eng., 111 (1994), 283–303.
[6] R. Glowinski, T. W. Pan and J. Periaux, A fictitious domain method for external incompressible flow modeled by Navier-Stokes equations, Comput. Methods. Appl. Mech. Eng., 112 (1994), 133–148.
[7] R. Glowinski, T. W. Pan and J. Periaux, A Lagrange multiplier/fictitious domain method for the Dirichlet problem, generalization to some flow problems, Japan J. Indust. Appl. Math., 12 (1995), 87–108.
[8] R. Glowinski, T. W. Pan, A. J. Kearsley and J. Periaux, Numerical simulation and optimal shape for viscous flow by a fictitious domain method, Int. J. Numer. Methods. Fluids., 20 (1995), 695–711.
[9] R. Glowinski, T. W. Pan, T. Hesla and D. D Joseph, A distributed Lagrange multiplier/fictitious method for flows around moving rigid bodies: application to particulate flows, Int. J. Multiphase. Flow., 25 (1999), 755–794.
[10] T. W. Pan, R. Glowinski and G. P. Galdi, Direct simulation of the motion of settling ellipsoid in Newtonian fluid, J. Comp. Appl. Math., 149 (2002), 71–82.
[11] J. L. Lions, Virtual and effective control for distributed systems and decomposition of everything, Journal d'Analyse Mathématique, 80(1) (2000), 257–297.

[12] R. Glowinski, Finite element method for incompressible viscous flow, In Handbook of Numerical Analysis, Vol. IX, P. G. Ciarlet and J. L. Lions, eds., North-Holland, Amsterdam, 3–1176, 2003.

[13] R. Glowinski, J. L. Lions and J. He, Exact and Approximate Controllability for Distributed Parameter Systems: A Numerical Approach, Cambridge University Press, Cambridge, UK, 2008.